


## Article

# Antenna Booster Versus a Spiral Monopole Antenna for Single-Band Operation at 900 MHz

Bernat Oller <sup>1</sup>, Aurora Andújar <sup>2</sup> and Jaume Anguera <sup>1,2,\*</sup> <sup>1</sup> Telecommunication Engineering, Universitat Ramon LLull, 08022 Barcelona, Spain; bernat.oller@salle.url.edu<sup>2</sup> Ignion, 08174 Barcelona, Spain; aurora.andujar@ignion.io

\* Correspondence: jaume.anguera@ignion.io or jaume.anguera@salle.url.edu

**Abstract:** The number of devices connected to the internet has grown exponentially through the last decade, making IoT and connection worldwide more possible every year, enabling an incredible number of applications. This calls for better and more efficient methods for designing wireless devices. An efficient and small antenna is needed to ensure connectivity, range, and battery life. Under these circumstances, antenna booster technology is proposed, which uses a tiny component called an antenna booster to excite currents in the ground plane of the IoT device. This allows the antenna booster to be as small as 12 mm × 3 mm × 2.4 mm, representing only  $\sim\lambda/30$  at 863 MHz. The antenna booster is matched across the frequency range using a matching network. The paper compares an antenna booster and a monopole antenna regarding bandwidth for a design using a 120 mm × 60 mm ground plane in the 863 MHz to 928 MHz frequency range. Afterwards, the same designs are analysed when the ground plane size changes from 20 mm × 30 mm to 200 mm × 200 mm using steps of 10 mm to determine which approach can be reused across 53.8% of the ground planes with  $S_{11} < -6$  dB without making any changes to the antenna system; for contrast, the monopole antenna can be reused only 4.6%. In addition, the antenna booster features better total efficiencies of up to 2.3 dB. A physical prototype with the antenna booster validates the numerical analysis.

**Keywords:** IoT; antenna boosters; monopole antennas; matching network; ISM

**Citation:** Oller, B.; Andújar, A.; Anguera, J. Antenna Booster Versus a Spiral Monopole Antenna for Single-Band Operation at 900 MHz. *Electronics* **2023**, *12*, 2067. <https://doi.org/10.3390/electronics12092067>

Academic Editors: Yiming Huo and Flavio Canavero

Received: 10 January 2023

Revised: 11 March 2023

Accepted: 24 April 2023

Published: 30 April 2023



**Copyright:** © 2023 by the authors. Licensee MDPI, Basel, Switzerland. This article is an open access article distributed under the terms and conditions of the Creative Commons Attribution (CC BY) license (<https://creativecommons.org/licenses/by/4.0/>).

## 1. Introduction

The revolution of the Internet of Things (IoT) connected era enables an endless field to invent new applications for tracking devices, intelligent sensors and agriculture, smart home, etc. The connectivity, range, and battery longevity of those devices depend upon antennas.

Antennas for wireless devices mainly rely on shaping the geometry of the antenna to make them small enough to fit in the device and multiband to provide operation across several frequency bands [1–10]. Spiral, meander, and loops are typical for designing an antenna to a particular frequency. In [11], a meandered monopole is proposed for a mobile phone. Although the bandwidth is 101.7%, the size is too big (100 mm × 44 mm,  $0.3\lambda$  at 900 MHz) to fit in a small IoT device (Table 1). In [12], a spiral monopole is proposed for covering 900 MHz, 1800 MHz, and 2200 MHz, having a size of 24 mm × 22.75 mm ( $\lambda/14$  at 900 MHz). In [13], a meandered monopole is designed for 900 MHz, with a large size of 42.2 mm × 70 mm ( $0.21\lambda$  at 900 MHz). In [14], a multi-spiral monopole is analysed for 900 MHz, with a size of 22.9 mm × 10 mm ( $\lambda/14$  at 900 MHz). In some cases, a simple matching network comprising lumped components such as capacitors and inductors is used for fine-tuning the frequency response of the antenna. Other cases use a tuneable component, such as a digitally tuneable capacitor with a meandered monopole of a compact size of 20 mm × 18 mm [15].

**Table 1.** Comparison of several monopole antennas for 900 MHz.

| Size (mm) and Maximum Electrical Size ( $\lambda$ ) at 900 MHz | BW (SWR = 3%) | Realised Gain (dBi) | Ground Plane (mm) | Ref. |
|--|---------------|---------------------|-------------------|------|
| 100 × 44, 0.3 $\lambda$  | 101.7         | -                   | 100 × 44          | [11] |
| 24 × 22.7, 0.072 $\lambda$                                     | 7.6           | -                   | 40 × 39           | [12] |
| 42.2 × 70, 0.21 $\lambda$                                      | 7.5           | −0.97               |                   | [13] |
| 22.9 × 10, 0.0687 $\lambda$                                    | 3.5           | 2.2                 | 27 × 6            | [14] |
| 20 × 18, 0.06 $\lambda$  | 6.1           | 1.0                 | 75 × 18           | [15] |

A different approach is addressed by antenna boosters, a tiny non-resonant element, where the frequencies of operation are easily adjusted thanks to a matching network [16]. Such a design is addressed with matching network synthesis tools available in microwave simulators [17–19].

The paper compares a classic spiral monopole antenna and an antenna booster when operating at 900 MHz in a reference 120 mm × 60 mm ground plane. Then, the size of the ground plane is changed while keeping both antenna systems the same. The objective is to compare the reusability of both antenna designs for a wide set of ground planes. In the end, the higher the reusability, the simpler the antenna technique is for device designers, since a particular design can be reused across a wide set of cases without any further change in the antenna part, either in the antenna geometry or in the matching network. This is a novel way of comparing antenna technologies since most of the prior art focuses only on a given antenna in a particular device size. As a result, a new figure of merit is proposed, called *reuse*, which quantifies how much an antenna element can be reused according to a specific parameter. In this case, the reference parameter is an  $S_{11} < -6$  dB, as elaborated in the next sections.

This paper is structured as follows: The two antenna types are compared in Section 2. In Section 3, both antenna types are studied for different ground planes, from a small size of 20 mm × 30 mm to a big size of 200 mm × 200 mm. Then, a prototype for the antenna booster is fabricated and tested to validate the numerical analysis. Next, a discussion is given in Section 4. Finally, Section 5 concludes.

## 2. Antenna Booster and Monopole Antenna Designs

The aim is to compare the performance of the antenna booster technology and a monopole antenna under the same challenging conditions. In order to create these conditions, the clearance area of the ground plane is reduced to only 20 mm × 11 mm, so the extra 40 mm × 11 mm ground plane area could be used for other purposes, such as integrating more electronics. The frequency range is the ISM 863–928 MHz.

Before comparing the antenna booster and the monopole antenna, it is worth mentioning some characteristics of an antenna booster. An antenna booster is an electrically small conductive parallelepiped, typically less than  $\lambda/20$  at the lowest frequency of operation, where the correct location on a ground plane of a PCB (Printed Circuit Board) enables the excitation of currents and, as a result, achieves bandwidth and efficiency. Since it is electrically small, its impedance nature is reactive and capacitive. Therefore, a matching network is added to provide impedance matching. This fact offers flexibility since the matching network allows the designer to provide single-band or multiband operation to the device. Moreover, the design of a matching network is easily addressed by network synthesis, which makes the design process easy and fast, and it looks more like a microwave problem than an antenna design [17]. It is worth mentioning that such excitation of currents depends on the position of the antenna booster on the ground plane [17], the corner being the preferred position. Either way, such excitation has no impact on the electronics, for example, on the sensitivity of the device compared to a classic monopole antenna [20]. In fact, currents on the ground plane are also excited by other antennas, such as PIFA. The advantage is that those currents can be excited by an antenna booster that is ten times smaller.

Firstly, the antenna booster and monopole antenna designs have been simulated with a reference ground plane size of  $120 \text{ mm} \times 60 \text{ mm} + 40 \text{ mm} \times 11 \text{ mm}$  printed on an FR4 (Flame Retardant #4 epoxy) substrate, commonly employed in PCBs due to its competitive price (Figure 1) [21]. Electromagnetic simulations are performed with MoM (Method of Moments) software (IE3D). Once both designs have been adjusted for operation for the reference ground plane, different ground planes ranging from  $20 \text{ mm} \times 30 \text{ mm}$  to  $200 \text{ mm} \times 200 \text{ mm}$  (using steps of  $10 \text{ mm}$ ) are going to be tested with the same antenna and matching network to see how many could be reused with the same design, without having to redo the design for each size.

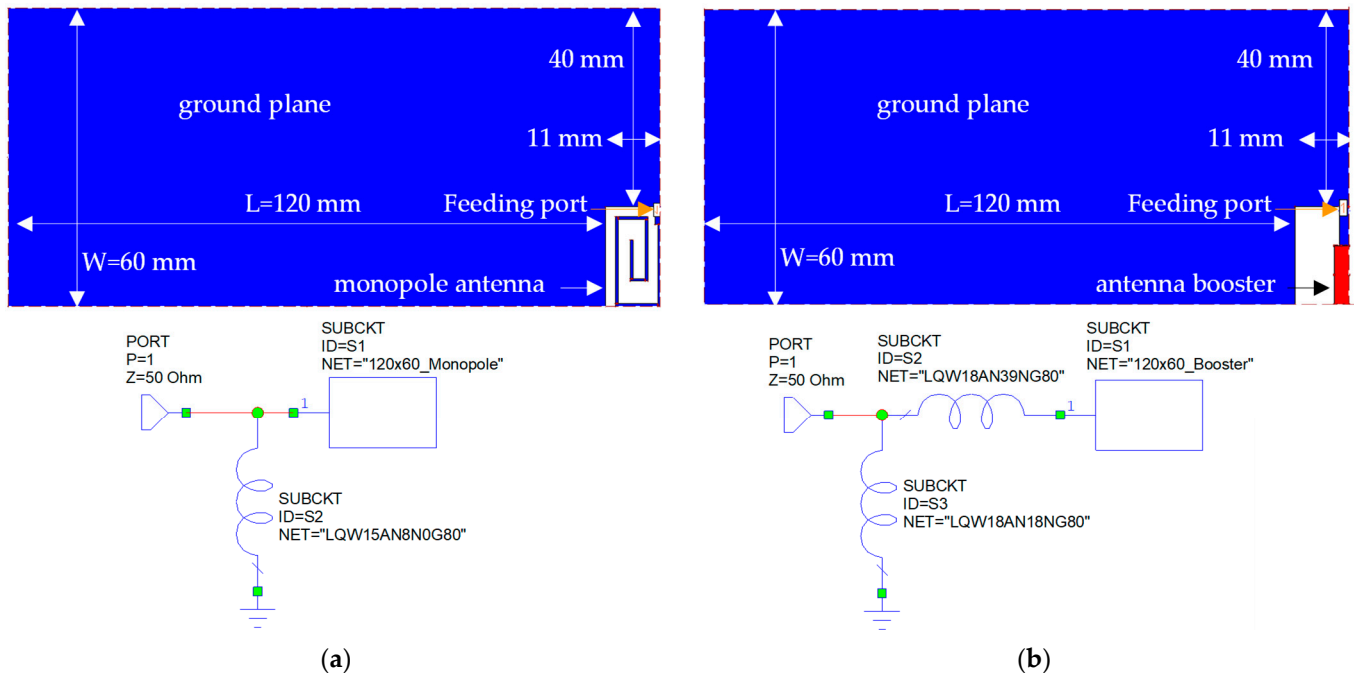


**Figure 1.** (a) Monopole antenna on a small clearance area of  $20 \text{ mm} \times 11 \text{ mm}$  with its matching network connected to a  $120 \text{ mm} \times 60 \text{ mm} + 40 \text{ mm} \times 11 \text{ mm}$  ground plane. (b)  $12 \text{ mm} \times 3 \text{ mm} \times 2.4 \text{ mm}$  (h) antenna booster on the same small clearance as the monopole. The ground plane (copper with  $\sigma = 5.9 \times 10^7 \text{ S/m}$ ) is printed on an FR4 substrate  $1 \text{ mm}$  thick,  $\epsilon_r = 4.15$ ,  $\tan\delta = 0.017$ .

The antenna design for the monopole antenna was obtained by adding a  $\lambda/4$  monopole to the ground plane and modifying its length to make it fit into the frequency band. The feeding point was placed on the added part of the ground plane to allow more bandwidth. Nevertheless, it was insufficient to match the band, so a matching network had to be added to fine-tune the impedance (Figure 1a). The matching network is a shunt inductor of value  $8 \text{ nH}$  (0402 SMD component,  $Q = 67$  at  $900 \text{ MHz}$ ).

As mentioned, the one-component matching network allows the impedance curve of the monopole antenna to stay below  $-6 \text{ dB}$ , which is the minimum required.

The second antenna design was based on the antenna booster technology [16,22]. Since the antenna booster is a non-resonant element, a matching network adds the flexibility to easily match the antenna system at the desired frequency [17]. Furthermore, since it is a single-band case, the matching network is simple, consisting of only two inductors (Figure 1b). This case consists of a series inductor of  $39 \text{ nH}$  and a shunt inductor of  $18 \text{ nH}$  ( $Q > 80$ ) (Figure 2). The feeding point is at the exact location of the monopole antenna, having the same  $20 \text{ mm} \times 11 \text{ mm}$  clearance area.

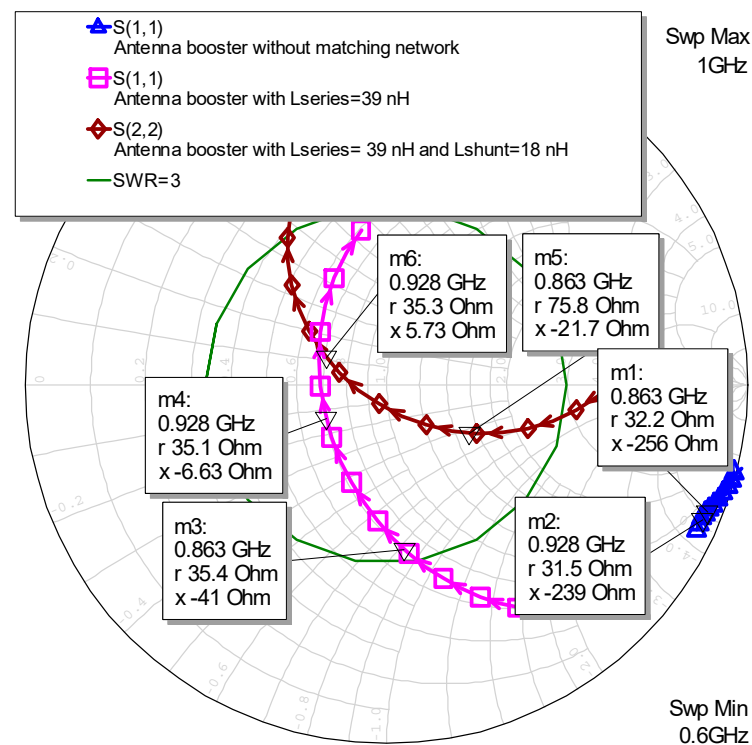


**Figure 2.** Steps to match the reactive capacitive impedance at 900 MHz of the antenna booster: a series and shunt inductance. The simulation considers the matching network of Figure 1 ( $L_{series} = 39$  nH,  $L_{shunt} = 18$  nH, including real component, i.e., finite Q).

Since the impedance of the antenna booster is capacitive, a series and a shunt inductor are used to match the antenna booster. As a result, the achieved bandwidth is  $BW = 17.4\%$ , 1.8 times the bandwidth achieved by the monopole antenna occupying the same clearance area (Figure 3, Table 2).

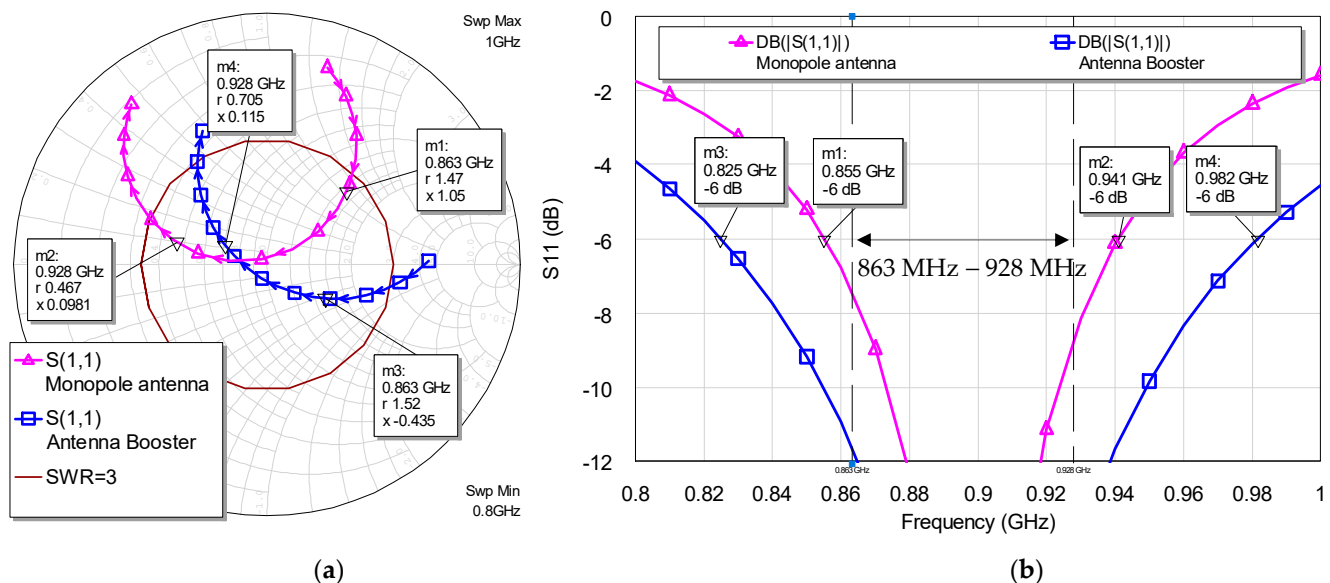


**Figure 3.** (a) Simulated input impedance for the monopole antenna and antenna booster, each with its matching network, as shown in Figure 1. (b) Simulated  $S_{11}$  of the monopole antenna and antenna booster showing that the antenna booster features 1.8 times more bandwidth.

**Table 2.** Bandwidth comparison for the cases shown in Figure 1.

| Antenna Element  | $f_1$ (GHz) | $f_2$ (GHz) | BW (% , $SWR \leq 3$ ) | Potential BW (% , $SWR \leq 3$ ) |
|------------------|-------------|-------------|------------------------|----------------------------------|
| Monopole antenna | 0.855       | 0.941       | 9.5                    | 9.4                              |
| Antenna Booster  | 0.825       | 0.982       | 17.4                   | 16.6                             |

To summarise the results of the antenna designs: they both accomplish 863–928 MHz. However, the antenna booster bandwidth is larger, making it more attractive since it can allocate more radio protocols beyond the 863–928 MHz frequency range. The bandwidth of both cases has been compared with bandwidth potential [23], with Optenni Lab results showing good agreement. Bandwidth potential considers the bandwidth an antenna can obtain with a simple matching network of one or two components. Having the antenna booster with more bandwidth enables a further reduction of the ground clearance area, which will imply only a new matching network. However, for the monopole antenna, a new antenna should be designed.

The following section analyses the impact of varying the ground plane size while keeping the same matching network. The purpose is to study the design reuse for other platforms without changing the matching network or the antenna part.

### 3. Analysis of the Reuse of the Antenna Systems for Different Ground Plane Sizes

The size of the ground plane is changed from a small one of 20 mm  $\times$  30 mm to 200 mm  $\times$  200 mm while keeping the same clearance area for both cases, being the same as the one for the reference 120 mm  $\times$  60 mm ground plane. The total number of ground planes is 342.

The worst reflection coefficient within the 863–928 MHz range is stored for each ground plane and then represented in a 2D plot. These results have been displayed in a thermal graph, where the warmer colours mean poor matching, and the cooler ones mean better matching ( $S_{11} \leq -6$  dB). Moreover, the edge with  $S_{11} = -6$  dB is defined using a black line (Figure 4). The ground planes providing an  $S_{11} \leq -6$  dB within 863–928 MHz are within the area inside the contours defined in Figure 4, called the *cluster*.

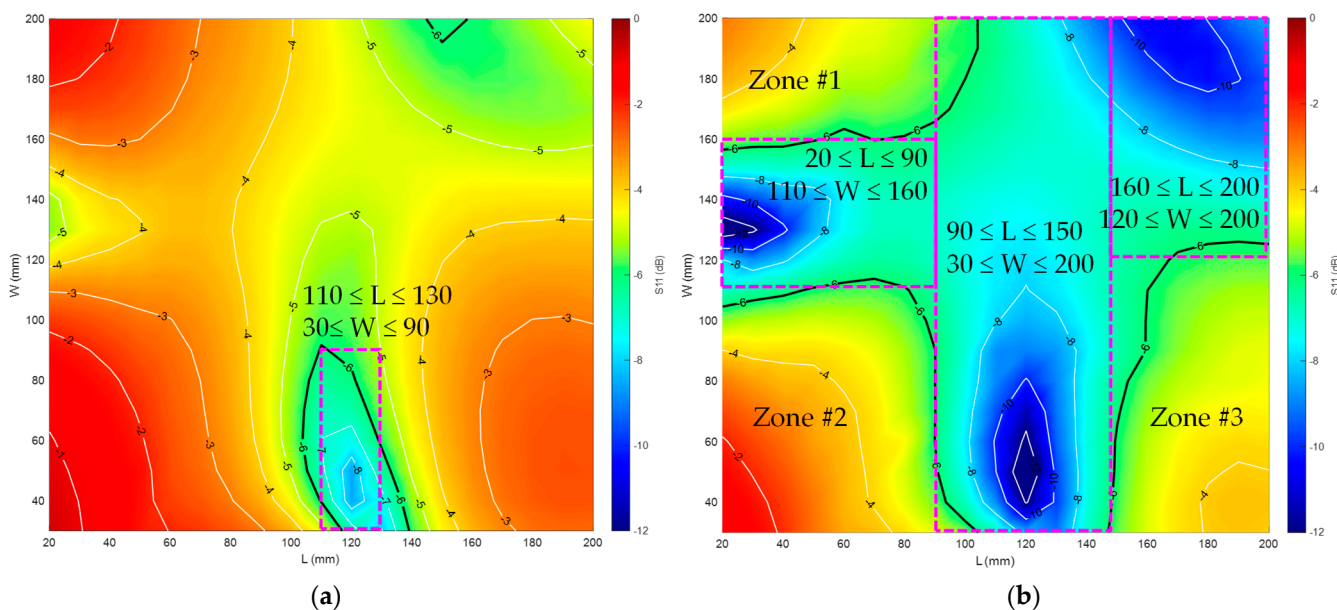


**Figure 4.** Worst  $S_{11}$  in the 863–928 MHz frequency range for the monopole antenna (a) and antenna booster (b) as a function of the length  $L$  and width  $W$  of the ground plane.



### 3.1. On the Reuse: The Cluster

Remarkably, the antenna booster is well-matched ( $S_{11} \leq -6$  dB) with many more different ground plane sizes than the monopole antenna (Figure 4, Table 3): the antenna booster can be reused across 53.8% cases, whereas the monopole antenna can be only reused 4.6%. For example, if the original 120 mm  $\times$  60 mm ground plane is reduced to 90 mm  $\times$  60 mm, the antenna booster maintains an  $S_{11} \leq -6$  dB across 863–928 MHz, whereas the monopole antenna degrades to  $-4$  dB. It is clearly shown from the cluster shapes (Figure 4) that the antenna booster is robust to ground plane changes, whereas the monopole is sensitive to changes.

**Table 3.** Reuse of each antenna system across the 342 different ground planes from 20 mm  $\times$  30 mm to 200 mm  $\times$  200 mm at steps of 10 mm. Reuse gathers how many cases from the total provide an  $S_{11} \leq -6$  dB across 863–928 MHz keeping the antenna system the same (same antenna element and same matching network).

| Antenna System   | Reuse (%) |
|------------------|-----------|
| Monopole antenna | 4.6       |
| Antenna Booster  | 53.8      |

The shape of the impedance cluster of the antenna booster is interesting, where it can be extrapolated to a cross delimited by the  $-6$  dB curve since the antenna is matched inside this zone. Moreover, as mentioned earlier, the reference case was designed on a 120 mm  $\times$  60 mm ground plane, which is why the coldest zones (better matching) are where  $L = 120$  mm and  $W = 60$  mm or vice versa, resulting in a symmetric cluster along the  $L = W$  line. The worst ground plane sizes are those in the corners, except the top right corner. The top left (large widths) and the bottom right (large lengths) parts, although not providing an  $S_{11} < -6$  dB with the current Lseries-Lshunt matching network, can be matched using a different matching network. However, the most critical area is the bottom left corner which includes electrically small ground planes. Further discussion on the off-cluster zones (Zone #1, 2, 3) can be found in [24]. In particular, Zone #1 and #3 need a different matching topology (antenna booster connected to a series L and shunt C). Zone #2 (small PCB) requires special treatment since the bandwidth decreases when the ground plane becomes smaller. Therefore, broad-banding mechanisms or reconfigurable solutions are needed to achieve bandwidth.

The total efficiency is computed for each ground plane size (Figure 5). Total efficiency considers both matching and radiation efficiency ( $\eta_r$ ) as follows,  $\eta_t = \eta_r(1 - |S_{11}|^2)$ , and represents the ratio of the radiated power to space over the incoming power to the antenna system. The simulation considers the losses due to the loss tangent of the substrate, the losses of the matching network, and the radiation efficiency of each antenna system on its respective ground plane size. The same matching network, as shown in Figure 1, is used. The total efficiency is superior for the antenna booster case. For example, for a 20 mm  $\times$  80 mm ground plane size, the antenna booster is 2.3 dB above the efficiency of the monopole.

Other values for different ground plane sizes are shown in Table 4. Besides this superior efficiency of the antenna booster compared to the monopole antenna, the better impedance matching when connecting the antenna booster to a transceiver ensures output power close to the nominal. Therefore, a side effect of mismatching besides total efficiency is its impact on the output power of the transceiver. As reflected in Figure 4, the antenna booster is more robust also in this regard, as the reuse ratio reflects.

The present result showing the better performance of the antenna booster compared to a monopole for small ground plane clearance is aligned with a different analysis where the same antenna booster presented here (12 mm  $\times$  3 mm  $\times$  2.4 mm) was compared for multiband performance to a large 96 mm  $\times$  21 mm FPC (Flexible Printed Circuit) antenna.

The conclusions of [25] were the superior performances in measured total efficiency for a small (65 mm × 42 mm), medium (95 mm × 42 mm), and large PCB (131 mm × 60 mm).

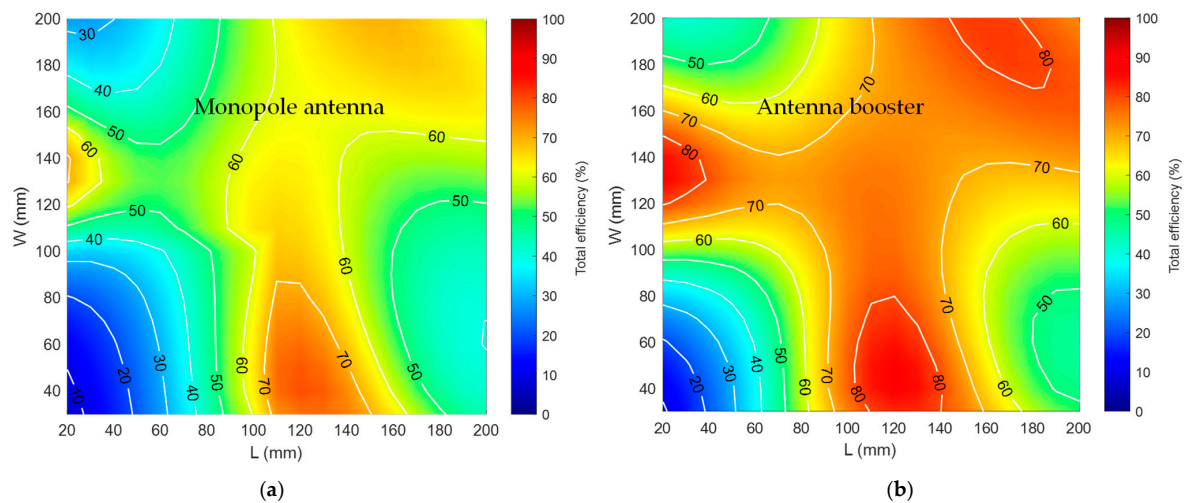


**Figure 5.** Simulated total efficiency considering the losses on the PCB (copper conductor and FR4 substrate), the losses of the matching network due to the lumped components with finite  $Q$  and the radiation efficiency as a function of the ground plane size  $L \times W$ . (a) monopole; (b) antenna booster.

**Table 4.** Comparison of total efficiencies averaged between 863 MHz and 928 MHz.

| Ground Plane Size $L \times W$ (mm) | Average Total Efficiency Monopole Antenna (%) | Average Total Efficiency Antenna Booster (%) | $\Delta$ (dB) |
|-------------------------------------|---|--|---------------|
| 60 × 60                             | 30.6  | 40.7   | 1.2           |
| 90 × 60                             | 55.6  | 68.7   | 0.9           |
| 120 × 60                            | 76.7  | 84.9   | 0.4           |
| 40 × 90                             | 28.4  | 45.8   | 2.0           |
| 180 × 180                           | 67.1  | 80.8   | 0.8           |

### 3.2. Physical Validation

After obtaining the results from the theoretical study, an experimental validation was conducted to validate the simulations (Figure 6). Two cases were fabricated and tested: the reference 120 mm × 60 mm ground plane and the 100 mm × 60 mm size. According to Figure 4, the 100 mm × 60 mm is within the cluster, and thus,  $S_{11}$  should be less than  $-6$  dB across 863–928 MHz. The measured data confirm this fact (Figure 7).

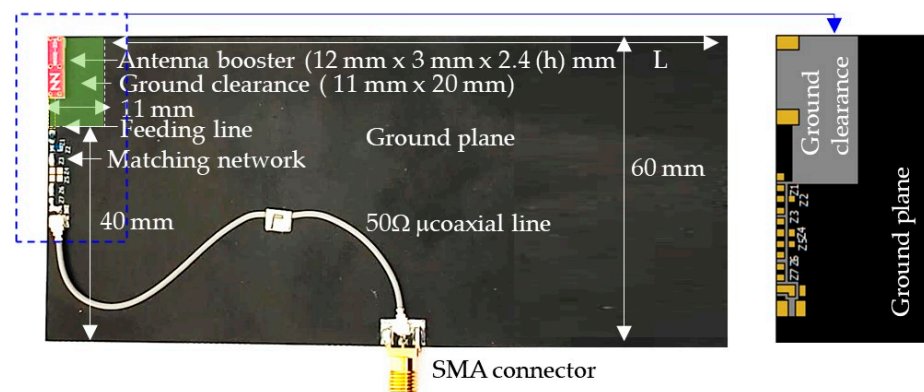


**Figure 6.** The prototype includes the 12 mm × 3 mm × 2.4 (h) mm antenna booster with a 20 mm × 11 mm ground clearance, the Lseries-Lshunt matching network, a ground plane with  $L \times 60$  mm, and an extension of 40 mm × 11 mm. In this case,  $L = 120$  mm. The ground plane is printed on an FR4 substrate (1 mm thick,  $\epsilon_r = 4.15$ ,  $\tan\delta = 0.017$ . PCB is 131 mm × 60 mm.

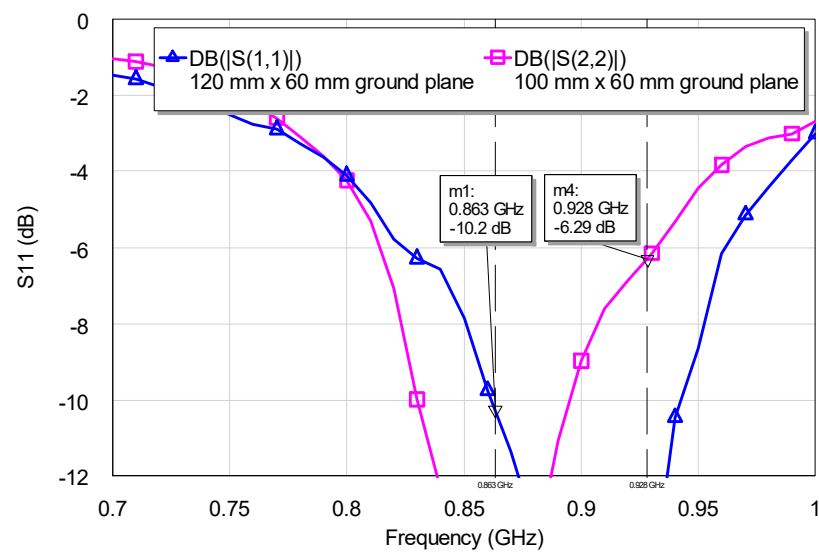


**Figure 7.** Measured  $S_{11}$  for the 120 mm  $\times$  60 mm (blue) and 100 mm  $\times$  60 mm (pink) ground planes with the same matching network. As predicted by the cluster (Figure 4a), both cases feature an  $S_{11} \leq -6$  dB across 863–928 MHz.

Moreover, the total antenna efficiency ( $\eta_t$ ) of the simulated and measured antenna is also displayed in Figure 8, showing good agreement. The simulated total efficiency across 863–928 MHz is 84%, while the measured is 76%, representing a 0.4 dB discrepancy, which is tolerable. Total efficiency is measured in the anechoic chamber using 3D pattern integration with MVG StarLab 18. Regarding realised gain, it reaches 2.8 dBi at 900 MHz, showing an omnidirectional pattern at XZ ( $\varphi = 0^\circ$  plane) and a drop along the long axis of the ground plane ( $\pm y$  direction). The radiation pattern is similar to a half-wavelength dipole, which is a consequence of the currents on the ground plane, which are aligned along the Y-axis for this ground plane size. This radiation pattern is convenient for IoT devices since the device receives almost equally from any direction of the incoming electromagnetic signal.

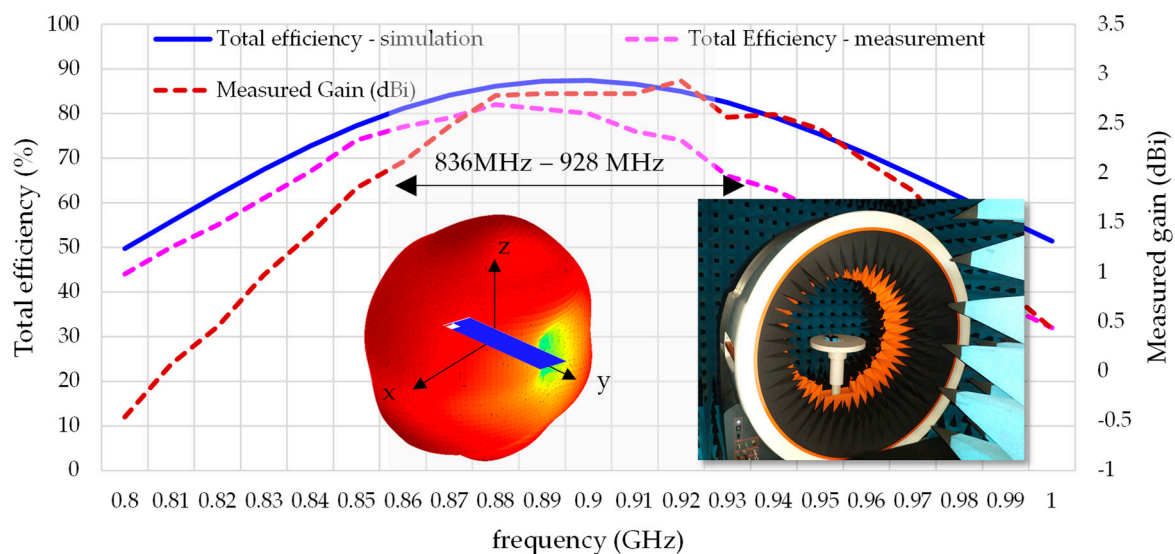
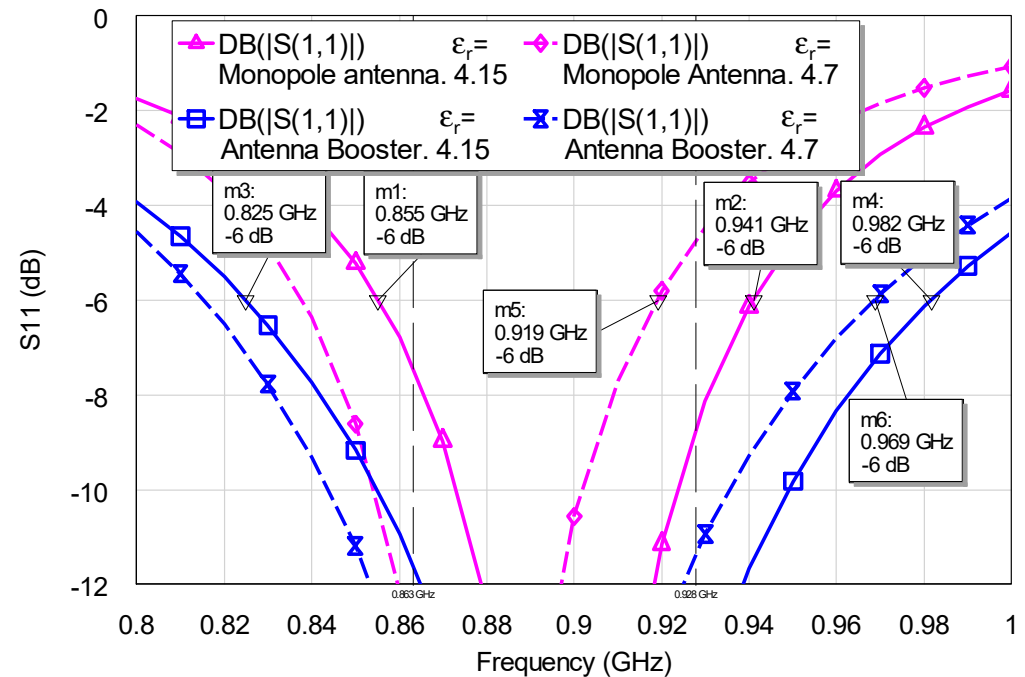


**Figure 8.** Simulated and measured total efficiency ( $\eta_t$ ) for the antenna booster in the reference 120 mm  $\times$  60 mm ground plane. The device under test is placed at the centre of the arc (MVG StarLab 18). Measured realised gain for the reference 120 mm  $\times$  60 mm ground plane and the measured 3D realised gain pattern at 900 MHz. The 3D pattern is represented in dB with a 30 dB dynamic range where the maximum is fixed at 2.8 dBi (the realised gain at 900 MHz).



#### 4. Discussion

Besides the previous advantages shown above, it is interesting to discuss the impact of the permittivity of the FR4 substrate since it may vary from manufacturer to manufacturer or due to temperature and humidity conditions [26]. In this case, the relative permittivity of the substrate of the PCB has been changed from the original 4.15 value to 4.7 while keeping everything else the same, including the matching networks (Figure 9).

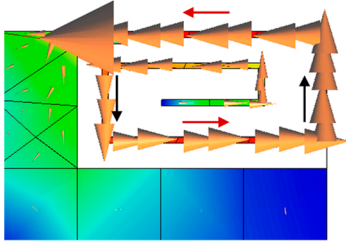
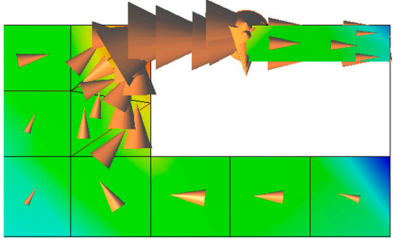


**Figure 9.** Impact on  $S_{11}$  when changing the  $\epsilon_r$  of the PCB substrate from the original 4.15 (continuous lines) value to 4.7 (discontinuous lines).

The  $S_{11}$  response for both the monopole antenna and antenna booster shift, as expected, to lower frequencies. However, the shifting is more accentuated for the monopole antenna, being 2.3% compared to 1.3% for the antenna booster. The reason is that the monopole antenna is more sensitive to changes in the permittivity of the substrate where the antenna is printed since it alters the coupling between the conductive parts of the antenna. However, the antenna booster being a single conductive element, it is more robust to substrate changes.

The main features of the monopole antenna compared to the antenna booster are gathered in Table 5. It is remarkable that in addition to the higher reuse of the antenna booster compared to the monopole antenna, the antenna booster can be reused if the ground clearance is further reduced. Since the antenna booster is only  $12 \text{ mm} \times 3 \text{ mm} \times 2.4 \text{ mm}$ , ground plane clearance can still be reduced. We must bear in mind that reducing the ground clearance reduces bandwidth. Still, as long as the bandwidth is enough for the application, such reduction may enable a larger integration of other components on the PCB. This is not the case for the monopole antenna. If the ground clearance reduces, the design process must start from scratch. For example, when the ground clearance is reduced from  $20 \text{ mm} \times 11 \text{ mm}$  ( $242 \text{ mm}^2$ ) to  $15 \text{ mm} \times 9 \text{ mm}$  ( $135 \text{ mm}^2$ ) for the reference  $120 \text{ mm} \times 60 \text{ mm}$  ground plane, the bandwidth of the antenna booster decreases from 17.4% to 11.5%. Although smaller, it is still better than the monopole antenna on the original clearance.

**Table 5.** Comparison between the monopole antenna and the antenna booster. The red and black arrows on the current distribution for the monopole antenna have been intentionally added to emphasise the out-of-phase currents. Ground plane clearance for both cases is 20 mm × 11 mm.

|  | Monopole Antenna  | Antenna Booster   |
|--|---|---|
| Current distribution at 900 MHz (The ground plane is partially shown; the ground plane is 120 mm × 60 mm for both cases) |  |                  |
| Reuse ( $S_{11} < -6$ dB)  | 4.6%  | 53.8%   |
| Total efficiency   | Lower due to out-of-phase current portions  | Higher (Figure 5, Table 4)  |
| BW (SWR = 3) at 900 MHz for a 120 mm × 60 mm ground plane  | 9.5%  | 17.4%   |
| Reduction of the clearance area  | Redesign the antenna geometry   | Only change the matching network  |
| Impact of the PCB substrate on frequency shifting when changing the $\epsilon_r = 4.15$ to 4.7                           | 2.3%  | 1.3%  |
| Design process   | Requires an iterative process   | Fast: the antenna booster is an off-the-shelf component, and also due to matching network synthesis |

## 5. Conclusions

A monopole antenna and an antenna booster have been compared when operating at 863 MHz to 928 MHz. Both solutions present an  $S_{11} \leq -6$  dB on this specific frequency band on the reference 120 mm × 60 mm ground plane. However, the antenna booster features more bandwidth at 900 MHz: 17.4% for the antenna booster compared to 9.5% for the monopole antenna. Therefore, the antenna booster can absorb new radio protocols beyond those in the 863–928 MHz frequency band.

Besides more bandwidth, another advantage of the antenna booster over the monopole antenna is its robustness to ground plane variations. A total of 342 ground planes ranging from 20 mm × 30 mm to 200 mm × 200 mm with increments of 10 mm have been used to analyse the performance of the monopole antenna and antenna booster. In all cases, the antenna set-up is the same: same antenna element and same matching network. The conducted analysis shows that the antenna booster can be reused 53.8%, whereas the monopole antenna only 4.6% (only for ground planes similar to the 120 mm × 60 mm reference ground plane). For example, the antenna booster system can be reused for ground planes with  $90 \text{ mm} \leq L \leq 150 \text{ mm}$  and  $30 \text{ mm} \leq W \leq 200 \text{ mm}$ ,  $20 \text{ mm} \leq L \leq 90 \text{ mm}$  and  $110 \text{ mm} \leq W \leq 160 \text{ mm}$ , and  $160 \text{ mm} \leq L \leq 200 \text{ mm}$  and  $120 \text{ mm} \leq W \leq 200 \text{ mm}$ . However, the monopole antenna can be reused for  $110 \text{ mm} \leq L \leq 130 \text{ mm}$  and  $30 \text{ mm} \leq W \leq 90 \text{ mm}$ , which is very limited compared to the antenna booster.

The antenna booster is also more robust to variations of the permittivity of the substrate due to different FR4s or changes in humidity or temperature affecting the permittivity. In this regard, when the relative permittivity changes from 4.15 to 4.7, the  $S_{11}$  response for the monopole antenna shifts 2.3% to lower frequencies, whereas the antenna booster is only 1.3%.

Keeping the bill of materials the same (same antenna booster and same matching network) reduces the time to design IoT devices and simplifies procurement and logistics.

**Author Contributions:** Conceptualization, B.O., A.A. and J.A.; Methodology, B.O., A.A. and J.A.; Writing—original draft, B.O. and J.A.; Writing—review & editing, B.O., A.A. and J.A.; Supervision, J.A. All authors have read and agreed to the published version of the manuscript.

**Funding:** This research received no external funding.

**Conflicts of Interest:** The authors declare no conflict of interest.

## References

- Wong, K.L. *Planar Antennas for Wireless Communications*; Wiley: Hoboken, NJ, USA, 2003.
- Rowell, C.; Lam, E.Y. Mobile-Phone Antenna Design. *IEEE Antennas Propag. Mag.* **2012**, *54*, 14–34. [\[CrossRef\]](#)
- Anguera, J.; Andújar, A.; Huynh, M.C.; Orlenius, C.; Picher, C.; Puente, C. Advances in Antenna Technology for Wireless Handheld Devices. *Int. J. Antennas Propag.* **2013**, *2013*, 838364. [\[CrossRef\]](#)
- Zheng, M.; Wang, H.; Hao, Y. Internal Hexa-Band Folded Monopole/Dipole/Loop Antenna with Four Resonances for Mobile Device. *IEEE Trans. Antennas Propag.* **2012**, *60*, 2880–2885. [\[CrossRef\]](#)
- Wang, Y.; Du, Z. Wideband Monopole Antenna with Less Nonground Portion for Octa-Band WWAN/LTE Mobile Phones. *IEEE Trans. Antennas Propag.* **2016**, *64*, 383–388. [\[CrossRef\]](#)
- Huang, D.; Du, Z.; Wang, Y. An Octa-band Monopole Antenna with a Small Nonground Portion Height for LTE/WLAN Mobile Phones. *IEEE Trans. Antennas Propag.* **2017**, *65*, 878–882. [\[CrossRef\]](#)
- Elsheikh, D.M.; Abdallah, E.A. Compact Multiband Multifolded-Slot Antenna Loaded With Printed-IFA. *IEEE Antennas Wirel. Propag. Lett.* **2012**, *11*, 1478–1481. [\[CrossRef\]](#)
- Wu, D.; Cheung, S.W.; Yuk, T.I. A compact and low-profile loop antenna with multiband operation for ultra-thin smartphones. *IEEE Trans. Antennas Propag.* **2015**, *63*, 2745–2750. [\[CrossRef\]](#)
- Shin, G.; Park, J.; Park, T.; Yoon, I. Compact 900-MHz LoRa Band Antenna on a Low-Profile AMC Surface. In Proceedings of the 2019 International Symposium on Antennas and Propagation (ISAP), Xi'an, China, 27–30 October 2019; pp. 1–2.
- Xu, Z.-Q.; Zhou, Q.-Q.; Ban, Y.-L.; Ang, S.S. Hepta-Band Coupled-Fed Loop Antenna For LTE/WWAN Unbroken Metal-Rimmed Smartphone Applications. *IEEE Trans. Antennas Propag.* **2018**, *17*, 311–814. [\[CrossRef\]](#)
- Zuo, S.-L.; Zhang, Z.-Y.; Yang, J.-W. Planar Meander Monopole Antenna With Parasitic Strips and Sleeve Feed for DVB-H/LTE/GSM850/900 Operation in the Mobile Phone. *IEEE Antennas Wirel. Propag. Lett.* **2013**, *12*, 27–30. [\[CrossRef\]](#)
- Ge, Y.; Esselle, K.P.; Bird, T.S. A Spiral-Shaped Printed Monopole Antenna for Mobile Communications. In Proceedings of the 2006 IEEE Antennas and Propagation Society International Symposium, Albuquerque, NM, USA, 9–14 July 2006; pp. 3681–3684. [\[CrossRef\]](#)
- Ahammed, M.D.J.; Praveena, R. Efficiency in Bandwidth by using Meander Line Antennas Simulation. *Int. J. Innov. Technol. Explor. Eng. (IJITEE)* **2019**, *9*. [\[CrossRef\]](#)
- Andrade, M.; Freire, R.C.S.; Fernandes, P.; Santana, E.E.C.; Santos, E.F.D.; de Souza, M.G.A.; Souza, A.S.; Serres, A.J.R. Compact Monopole Antenna for Smart Meter Applications in ISM Band 900 MHz. In Proceedings of the 23rd International Workshop on ADC and DAC Modelling and Testing IMEKO TC-4 2020, Brescia, Italy, 12–14 September 2022.
- Ferrero, F.; Trinh, L.H. 868MHz Antenna Input Impedance Reconfiguration for IoT applications. In Proceedings of the 2022 IEEE Conference on Antenna Measurements and Applications (CAMA), Guangzhou, China, 14–17 December 2022; pp. 1–2. [\[CrossRef\]](#)
- Anguera, J.; Andújar, A.; Puente, C.; Mumbrú, J. Antennaless Wireless Device Capable of Operation in Multiple Frequency Regions. US Patent 8736497, 4 August 2008.
- Anguera, J.; Andújar, A.; Mestre, G.; Rahola, J.; Juntunen, J. Design of Multiband Antenna Systems for Wireless Devices Using Antenna Boosters. *IEEE Microw. Mag.* **2019**, *20*, 102–114. [\[CrossRef\]](#)
- Vye, D. Network Synthesis Wizard Automates Interactive Matching-Circuit Design. *Microw. J.* **2018**, *61*, 96–102.
- Rahola, J. Optimization of matching circuits for antennas. In Proceedings of the European Conference on Antennas and Propagation, EuCAP 2011, Rome, Italy, 11–15 April 2011.
- Anguera, J.; Andújar, A.; Puente, C. Antenna-Less Wireless: A Marriage between Antenna and Microwave Engineering. *Microw. J.* **2017**, *60*, 22–36.
- Aguilar, J.R.; Beadle, M.; Thompson, P.T.; Shelley, M.W. The microwave and RF characteristics of FR4 substrates. In Proceedings of the IEE Colloquium on Low Cost Antenna Technology (Ref. No. 1998/206), London, UK, 24 February 1998; pp. 2/1–2/6. [\[CrossRef\]](#)
- Anguera, J.; Toporcer, N.; Andújar, A. Slim Radiating Systems for Electronic Devices. US Patent US9960478 (B2), 4 July 2018.
- Rahola, J. Bandwidth potential and electromagnetic isolation: Tools for analyzing the impedance behaviour of antenna systems. In Proceedings of the EuCAP 2009 Conference, Berlin, Germany, 23–27 March 2009.
- Gui, J.; Andújar, A.; Anguera, J. On the reuse of a matching network for IoT devices operating at 900 MHz embedding antenna boosters. *Electronics* **2022**, *11*, 1267. [\[CrossRef\]](#)
- Anguera, J.; Fernández, A.; Puente, C.; Andújar, A.; Groot, J. Antenna Boosters versus Flexible Printed Circuit Antennas for IoT Devices. *Signals* **2022**, *3*, 326–340. [\[CrossRef\]](#)

26. Beyene, W.T.; Cheng, N.; Feng, J.; Shi, H.; Oh, D.; Yuan, C. Performance analysis of multi-gigahertz parallel bus with transmit pre-emphasis equalization. In Proceedings of the IEEE MTT-S International Microwave Symposium Digest, Long Beach, CA, USA, 12–17 June 2005; pp. 1849–1852. [[CrossRef](#)]

**Disclaimer/Publisher’s Note:** The statements, opinions and data contained in all publications are solely those of the individual author(s) and contributor(s) and not of MDPI and/or the editor(s). MDPI and/or the editor(s) disclaim responsibility for any injury to people or property resulting from any ideas, methods, instructions or products referred to in the content.